

# Biomimetic Fabrication of Pseudo-hexagonal Aragonite Tablets Through a Temperature-Varying Approach

Fenglin Liu,<sup>a</sup> Yanyan Gao,<sup>a</sup> Shiqiang Zhao,<sup>a</sup> Qiang Shen,<sup>\*a</sup> Yunlan Su<sup>b</sup> and Dujin Wang<sup>b</sup>

## S1. Experimental Section

All chemicals, sodium dodecyl sulfate (SDS), calcium chloride, magnesium chloride, and ammonium bicarbonate, are of A. R. grade and were used without further purification. Deionized water was used throughout the sample preparations. The two-tailed anionic surfactants of calcium dodecyl sulfate  $\text{Ca}(\text{DS})_2$  and magnesium dodecyl sulfate  $\text{Mg}(\text{DS})_2$  were synthesized using the precipitation reactions of SDS with calcium chloride and magnesium chloride at a proper temperature, respectively.

Prior to each experiment, the aqueous solutions of  $(\text{NH}_4)_2\text{CO}_3$  (10.00–100.00 mM) and  $\text{M}(\text{DS})_2$  ( $[\text{Ca}^{2+}] + [\text{Mg}^{2+}] = 10.00\text{--}100.00$  mM, Ca/Mg molar ratios = 10:0, 9:1, 8.75:1.25, 8:2, or 5:5) were freshly prepared at room temperature and at 60°C, respectively. Then, a 50 mL of surfactant solution was transferred into a 200-mL beaker, placed in a 60°C water-bath and agitated at a constant rate of 1300 rpm by means of a Teflon-coated magnetic stirring-bar. After the dropwise adding of the equal molarity of  $(\text{NH}_4)_2\text{CO}_3$  solution (50 mL), the reaction system was kept at the stirring state for another 10 min. And then, the reaction system (pH = 8.0) was allowed to stand still in a 30°C thermostatic chamber for 1 day. Finally, after the removal of clear supernatant, the resulting precipitates were rinsed three times with the mixture of ethanol and water (50:50, v/v), dried at 30°C for 1 day, and then used for measurements.

The collected  $\text{CaCO}_3$  solids were Pt-coated prior to examination by a JEOL JSM-7600F scanning electron microscope (SEM), fitted with a field-emission source and operating at an accelerating voltage

of 15 kV. For Transmission Electron Microscopy (TEM) studies, the samples were ultrasonically dispersed in alcohol and then were manipulated by mounting a drop of the dispersion on a carbon coated Cu grid. The measurements were carried out by a JEM-100CX11 TEM operating at 100 kV and a high-resolution JEM-2100 TEM operating at 200 kV. The X-ray diffraction (XRD) patterns were performed on a Rigaku D/max-2400 powder X-ray diffractometer with Cu K $\alpha$  radiation (40 kV, 120 mA). The 0.02° steps/(25 s) and the 2 $\theta$  range from 20 to 60° were selected to analyze the crystal structure and orientation. Nitrogen adsorption–desorption measurements were carried out on a Coulter Omnisorp 100CX gas adsorption analyzer. The CaCO<sub>3</sub> samples (0.5~1.0 g) were degassed at 350°C for 4 h under a pressure of 10<sup>-5</sup> Pa or below. The surface area was calculated using the BET method in a relative pressure (P/P<sub>0</sub>) range of 0.05–0.25. The pore size distribution was evaluated using the Barret–Joyner–Halenda (BJH) model.

## S2. Fabrication of Aragonite

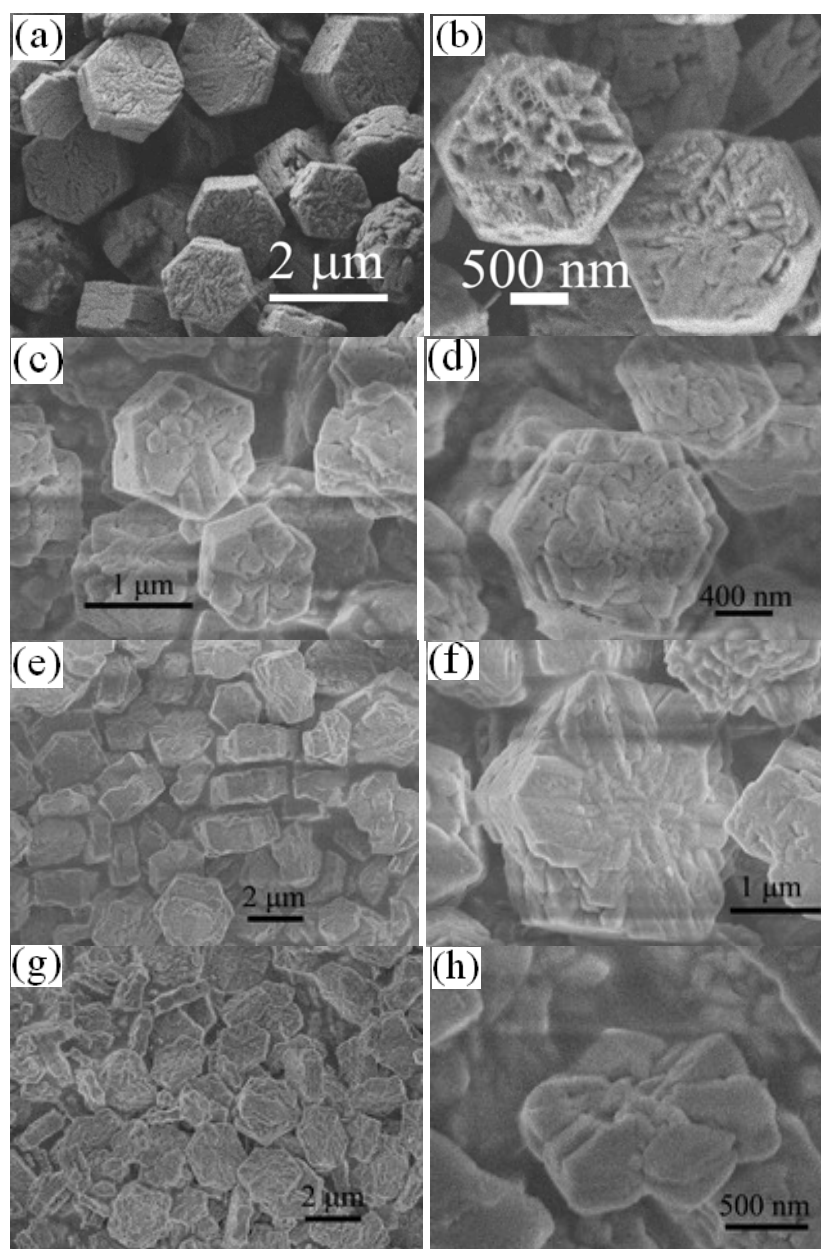


**Fig.S1.** SEM images of various aragonite tablets sampled from the reaction systems of  $M(DS)_2$  (Ca/Mg molar ratio = 5:5) at various surfactant concentrations: (a, b) 5.0; (c, d) 8.0; (e, f) 10.0; and (g, h) 50.0 mM.

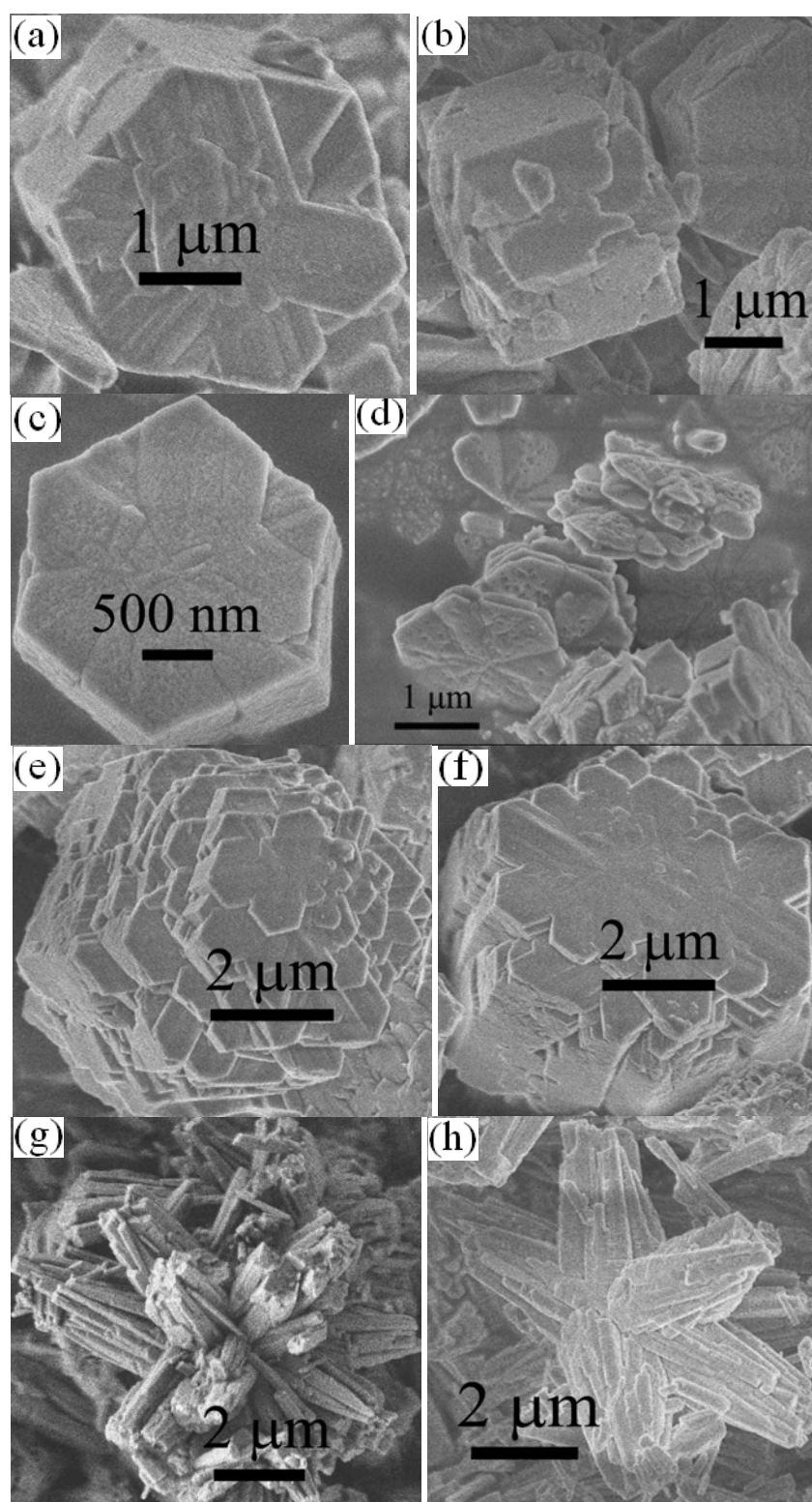


**Fig.S2.** SEM images of various aragonite representatives sampled from the different divalent metal-ion sources of calcium and magnesium ( $[\text{Ca}^{2+}] + [\text{Mg}^{2+}] = 5 \text{ mM}$ , Ca/Mg molar ratio = 8:2): (a, b)  $\text{Ca}(\text{DS})_2 + \text{Mg}(\text{DS})_2$ ; (c, d)  $\text{Ca}(\text{DS})_2 + \text{MgCl}_2$ ; (e, f)  $\text{CaCl}_2 + \text{Mg}(\text{DS})_2$ ; and (g, h)  $\text{CaCl}_2 + \text{MgCl}_2$ .

### S3. Properties of Tabular Aragonite

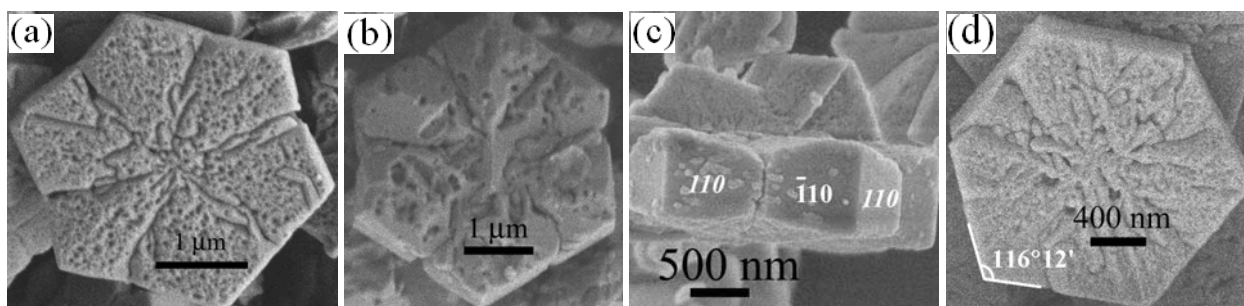


**Fig.S3.** SEM images of representative aragonite particles obtained from the reaction systems of  $M(DS)_2$  ( $[Ca^{2+}] + [Mg^{2+}] = 5 \sim 50$  mM, Ca/Mg molar ratio = 5:5), showing the triplet twinning nature and pseudo-hexagonal appearance of mature aragonite tablets. According to the triple twinning nature of aragonite, the side planes of  $\{110\}$  were marked in panel (c). The interfacial angle between  $(-110)$  and  $(110)$  planes of orthorhombic aragonite is  $63^\circ 48'$ , the supplementary angle (i.e.,  $116^\circ 12'$ ) of which was marked in panel (d). Panel (d) shows also the seemingly single-crystalline nature of a pseudo-hexagonal tablet.

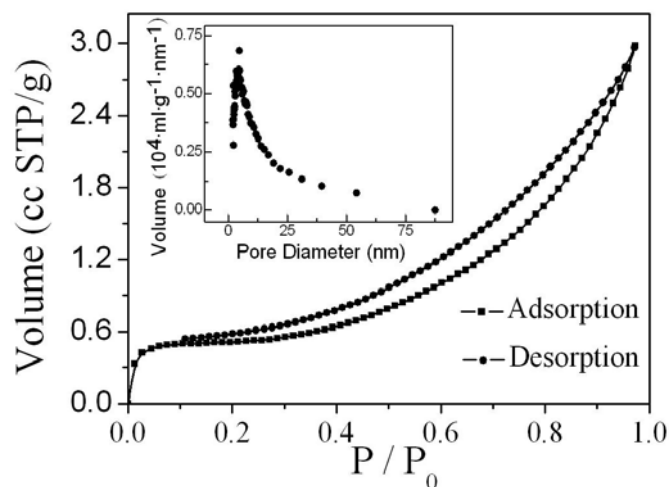


**Fig.S4.** Nitrogen adsorption-desorption of pseudo-hexagonal aragonite crystals obtained from the reaction systems of 5 mM  $M(DS)_2$  (Ca/Mg molar ratio = 5:5) at the reaction time of 24 h. Inset is the corresponding pore size distribution curve. The calculated average Brunauer-Emmett-Teller (BET) surface area was  $3.6 \pm 1.0$   $m^2 \cdot g^{-1}$ , and the calculated pore size was  $3.8 \pm 0.8$  nm. These extremely low values indicate that the so-called porosity of aragonite tablets might not be attributed to their mesoporous structure, but to the doping of amorphous  $CaCO_3$  and/or magnesium salts.

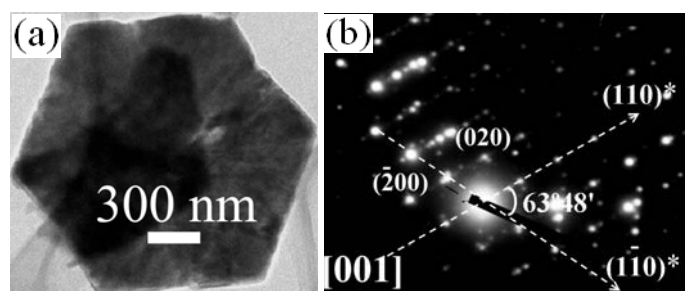


**Fig.S5.** (a) TEM image and (b) the corresponding SAED pattern of a growing aragonite tablet obtained from the reaction system of 5 mM  $M(\text{DS})_2$  at the Ca/Mg molar ratio of 5:5. According to the crystal phase and crystallographic orientation of aragonite, two diffraction spots, the zone axis of [001], the twinning planes of {110}, and the corresponding interfacial angle were marked in the SAED pattern.

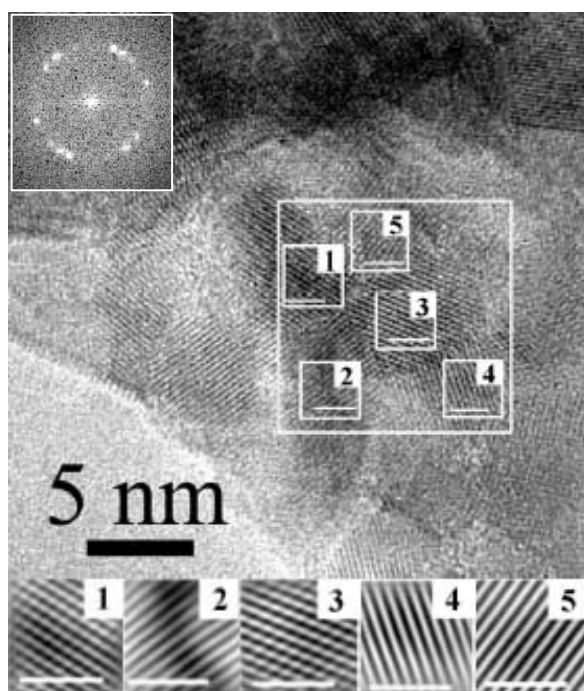


**Fig.S6.** High-resolution TEM image of a tabular aragonite intermediate. Inset is the SAED pattern of the relatively big rectangular region, indicating that the polycrystalline region was composed of several “single-crystalline” nanoparticles. Five rectangular regions (Scale bar = 1 nm) in the bigger one were magnified, filtered, and shown underneath. The filtered regions correspond to the aragonite lattice planes of (200) with an interplaner spacing of  $\sim 2.48 \text{ \AA}$ .

## S4. Formation Mechanism

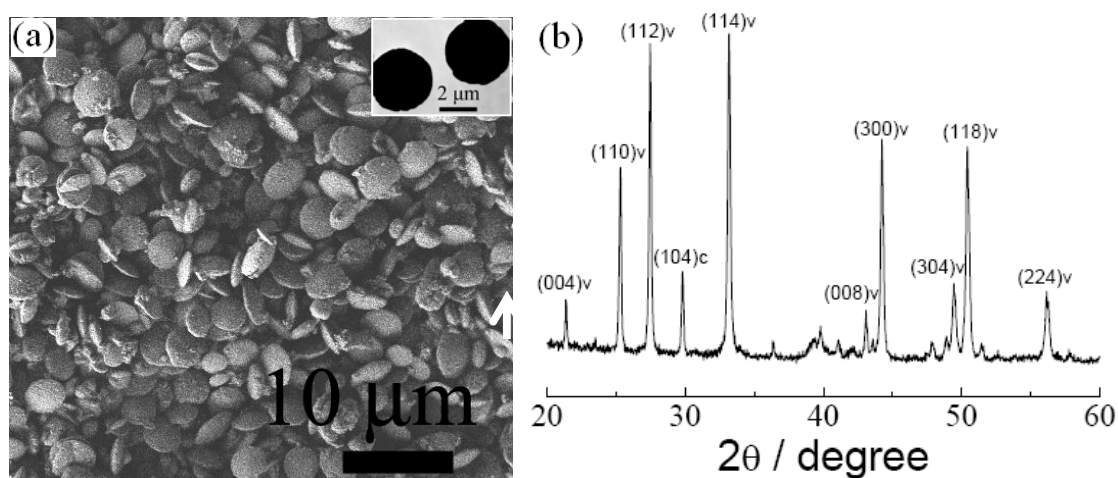


**Fig.S7.** (a) SEM image and (b) XRD profile of the  $\text{CaCO}_3$  crystals sampled from the reaction systems of 5 mM  $\text{Ca}(\text{DS})_2$ . Inset shows that there are no holes in the centers of vaterite particles. The subscripts v and c represent vaterite and calcite, respectively.

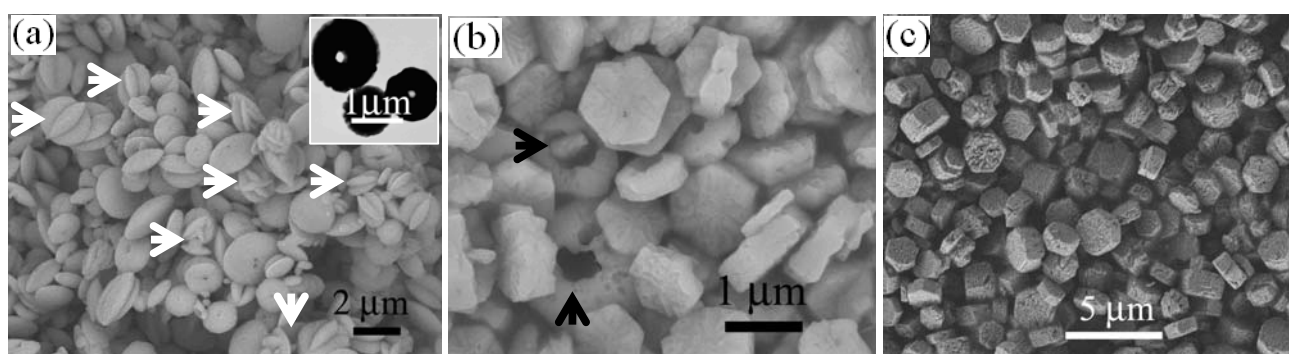


**Fig.S8.** SEM images of the  $\text{CaCO}_3$  crystals sampled from the reaction systems of  $\text{M}(\text{DS})_2$  at various Ca/Mg molar ratios: (a) 9:1, (b) 8:2, and (c) 5:5. Inset in panel a) shows the TEM picture of lens-shaped vaterite particles with a hole in the center.

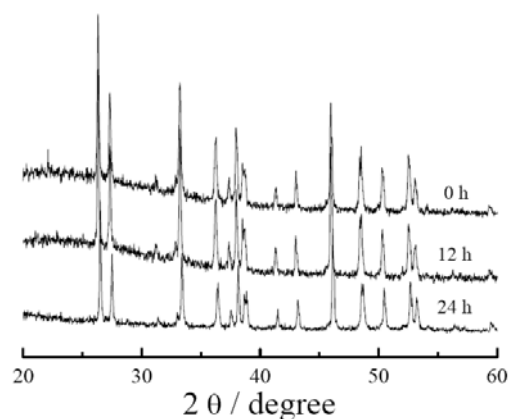


**Fig.S9.** XRD patterns of pseudo-hexagonal aragonite crystals obtained from the reaction systems of 5 mM  $M(\text{DS})_2$  (Ca/Mg molar ratio = 5:5) at the **aging** times of 0, 12, and 24 h. The broad hump-like baselines in the  $2\theta$  range of 20 and 35° indicate the existence of amorphous calcium carbonate at the **aging** times of 0 and 12 h.

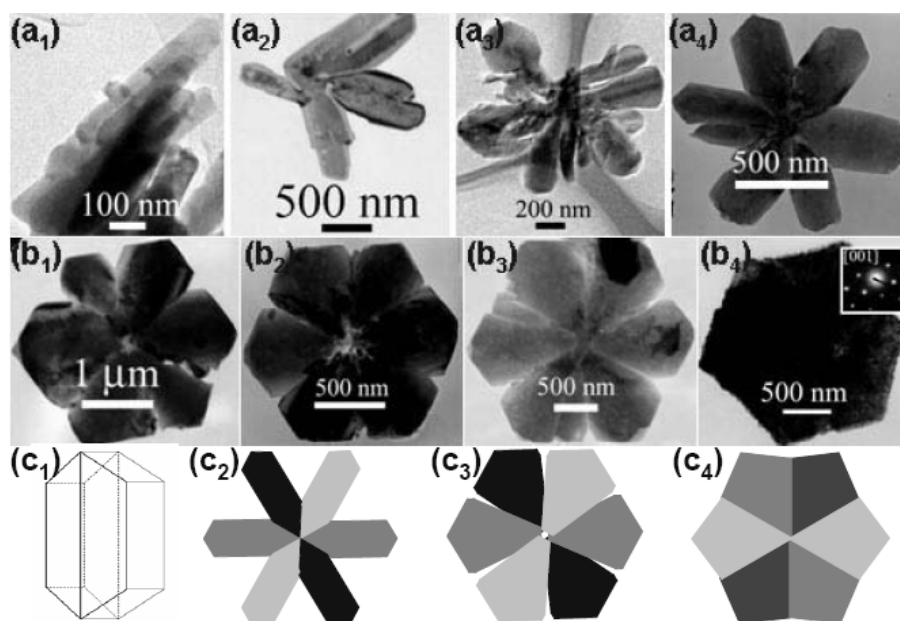


**Fig.S10.** (a, b) TEM images and (c) schematic drawings of growing aragonite particles suggest the interpenetration twinning mechanism of a single-crystal-like tablet: (a<sub>1</sub>-a<sub>4</sub>), the individual aragonite rods and their intergrowths; (b<sub>1</sub>-b<sub>4</sub>), the diagonal intergrowths of six petals and the developed pseudo-hexagonal tablet with a single-crystal-like nature; (c<sub>1</sub>-c<sub>4</sub>), the morphological evolution of a triplet twinning aragonite tablet.